THE JOURNAL OF PHYSICAL CHEMISTRY B

Article

pubs.acs.org/JPCB

Nanostructure–Thermal Conductivity Relationships in Protic Ionic Liquids

Thomas Murphy,[†] Luis M. Varela,[‡] Grant B. Webber,[†] Gregory G. Warr,[§] and Rob Atkin*[,†]

[†]Priority Research Centre for Advanced Particle Processing and Transport, The University of Newcastle, NSW 2308, Callaghan, Australia

[‡]Grupo de Nanomateriais e Materia Branda, Departamento de Física da Materia Condensada, Universidade de Santiago de Compostela, Campus Vida s/n E-15782, Santiago de Compostela, Spain

[§]School of Chemistry, The University of Sydney, Sydney, NSW 2006, Australia

ABSTRACT: The thermal conductivities of nine protic ionic liquids (ILs) have been investigated between 293 and 340 K. Within this range, the thermal conductivities are between 0.18 and 0.30 $W \cdot m^{-1} \cdot K^{-1}$. These values are higher than those typically associated with oils and aprotic ILs, but lower than those of strongly hydrogen bonding solvents like water. Weak linear decreases in thermal conductivity with temperature are noted, with the exception of ethanolammonium nitrate (EtAN) where the thermal conductivity increases with temperature. The dependence of thermal conductivity on IL type is analyzed with use of the Bahe–Varela pseudolattice theory. This theory treats the bulk IL as an array of ordered domains with intervening domains of uncorrelated structure which enable and provide barriers to heat propagation (respectively) via allowed vibrational modes. For the protic ILs investigated, thermal conductivity depends strongly on the IL cation alkyl chain length. This is because the cation alkyl chain controls the dimensions of the IL bulk nanostructure, which consists of charged (ordered domains) and uncharged regions (disordered domains). As the cation alkyl chain controls the dimensions of the disordered domains, it thus limits the thermal conductivity. To test the generality of this interpretation, the thermal conductivities of propylammonium nitrate (PAN) and PAN–octanol mixtures were examined; water selectively swells the PAN charged domain, while octanol swells the uncharged regions. Up to a certain concentration, adding water increases thermal conduction and octanol decreases it, as expected. However, at high solute concentrations the IL nanostructure is broken. When additional solvent is added above this concentration the rate of change in thermal conductivity is greatly reduced. This is because, in the absence of nanostructure, the added solvent only serves to dilute the salt solution.

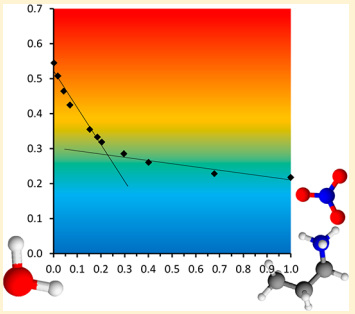

INTRODUCTION

Ionic liquids (ILs) are pure salts with melting points below 100 °C. ILs are divided into two general classes, differentiated by the mechanism of cation formation. Protic ILs are synthesized via proton transfer from a Brønsted acid to a Brønsted base[1,2] and aprotic ILs are formed by a charge transfer metathesis or quaternization reactions.[3,4] A key feature of protic ILs is their ability to form hydrogen bonds; some protic ILs are capable of forming extensive three-dimensional hydrogen bond networks. ILs are a promising solvent class due to their useful physicochemical properties.[5−8] These can include high electrochemical stability,[9,10] high thermal stability,[1,11] low vapor pressure,[12,13] nonflammability,[1,14] high volumetric heat capacity,[15,16] and high thermal conductivity.[16−20] These properties make ILs ideal candidates for next generation thermal fluids.

A remarkable feature of many ILs is the presence of structural inhomogeneity within the liquid bulk referred to as nanostructure.[21−26] Nanostructure is primarily the result of strong Coulombic interactions, sometimes bolstered by hydrogen bonding, between the charged groups of IL ions. These strong interactions produce extended charged domains with alkyl groups solvophobically segregated into apolar alkyl domains, often producing a bicontinuous L_3-sponge-like morphology of charged and alkyl domains.[2,21,23] Solvophobic nanostructure occurs in imidazolium-based ILs with alkyl chains $\geq C_4$,[25,27−29] while alkyl chains as short as C_2 are sufficiently long in primary ammonium based protic ILs.[22]

IL nanostructure influences properties including solvent strength,[30−32] viscosity,[33−36] interfacial structure,[3,37−39] the stability of nanoparticle dispersions,[40,41] and the ability to support amphiphilic self-assembly.[30,31] There is also evidence indicating that the acoustic properties of ILs are influenced by the segregation of alkyl and ionic domains within the bulk IL[42] which is important for this study because thermal conductivity and the speed of sound in a liquid are correlated.[43,44]

Thermal energy is conducted via different mechanisms in different materials. In a dilute gas, diffusive and collision processes dominate thermal transport as described by classical Chapman–Enskog kinetic theory.[45] In a solid, quantized, spatially extended lattice vibrational modes, called phonons, dominate thermal transport. Thermal transport behavior in

Received: July 23, 2014
Revised: September 17, 2014
Published: September 17, 2014

   dx.doi.org/10.1021/jp507408r | J. Phys. Chem. B 2014, 118, 12017−12024

Table 1. Thermal Conductivity (λ), Molar Mass (M), Viscosity (η), Density (ρ), Surface Tension (γ), and Melting Point (T_m)[a]

IL	λ, W·m^{-1}·K^{-1}	M, g·mol^{-1}	η, cP	ρ, g·cm^{-3}	γ, mN·m^{-1}	T_m, °C	repeat spacing, Å	cutoff frequency, ω_c, THz
BASCN	0.181	132	97.0[64]	0.949[64]	34.9	20.5[64]	13.2[65]	6.0
BAN	0.197	136	72.0[36]	1.10[36]	33.0[36]		14.2[26]	6.0
DMEAF	0.201	119	9.8[33]	1.03[3]	51.8			
EASCN	0.209	104		1.19		41[23]	10.1[65]	
PAN	0.218	122	89.3[33]	1.157[1]	40.0[36]	4[64]	11.9[65]	7.9
EAF	0.249	91	23.1[33]	1.039[66]	38.5[66]	−15[23]	10.0[65]	9.0
EAN	0.245	108	35.9[33]	1.216[66]	48.5[67]	12[23]	10.1[65]	9.0
EAHS	0.259	143	250.0	1.438[66]	56.3[66]	40[b,23]	10.0[65]	9.0
EtAN	0.295	124	156.0[33]	1.265[66]	72.1[67]	52[b,23]	8.21[65]	

[a]All values reported are at 293 K except for melting point. [b]EASCN, EAHS, and EtAN exist as metastable liquids.

liquids lies somewhere between that of solids and gases. Beginning with a dilute gas, as the density increases, the role of potential field interactions increases until, in the liquid regime, phonon-like vibrational modes dominate heat transfer and diffusive and collision contributions are relatively minor.[46,44,47] These modes are derived from the allowed oscillations of an atom or molecule about a potential minimum, which are described by harmonic theories of liquids.[44,47,48]

The Bahe−Varela pseudolattice theory[49,50] was originally developed to describe the behavior of concentrated electrolyte solutions, but has been shown to be applicable for aprotic ILs.[43,51,52] Like ILs, concentrated electrolyte solutions have intermediate-range order;[53,54] X-ray diffraction spectra of these solutions feature Bragg peaks like those produced by well-defined solid crystalline lattice structures. The Bahe−Varela theory conceptualizes the bulk liquid as a pseudolattice, comprised of an array of ordered domains separated by uncorrelated regions. Well-defined vibrational modes, including spatially extended low-frequency modes, can readily transport thermal energy throughout the pseudolattice by hopping between ordered domains across the uncorrelated structure. To hop across a barrier, the vibrational mode wavelength must be greater than the barrier width. This means that the characteristic size of the liquid's structure places a frequency limit on the vibrational modes able to propagate through its pseudolattice; this upper frequency cutoff is denoted ω_c.

The maximal ionic concentrations and well-established intermediate-range order (nanostructure) of ILs make them ideal systems for application of the Bahe−Varela theory.[43,51,52] The theory has already been applied to describe sorption processes at an IL/air interface,[52] the electrical conductivity of IL mixtures,[51] and, more recently, thermal conductivity.[43] In ILs, the ordered and disordered domains of the Bahe−Varela theory are equated with charged and uncharged domains. The size of the uncharged domains, which controls heat propagation, are determined by ion moiety dimensions and the correlation length of the IL nanostructure determined from scattering or diffraction peaks. The relative sizes of these domains are determined by the ion structures and they can be characterized by the repeat lengths characterizing an IL's nanostructure.[2,21]

In this work, relationships between thermal conductivity and protic IL nanostructure are determined and discussed in the context of the Bahe−Varela theory. The protic ILs examined are ethanolammonium nitrate (EtAN), ethylammonium nitrate (EAN), propylammonium nitrate (PAN), butylammonium nitrate (BAN), ethylammonium formate (EAF), dimethylethylammonium formate (DMEAF), ethylammonium hydrogensulfate (EAHS), ethylammonium thiocyanate (EASCN), and butylammonium thiocyanate (BASCN). Additionally, PAN−octanol and PAN−water mixtures are examined to confirm the role played by nanostructure in IL thermal transport.

MATERIALS AND METHODS

The ILs ethanolammonium nitrate (EtAN), ethylammonium nitrate (EAN), propylammonium nitrate (PAN), butylammonium nitrate (BAN), ethylammonium formate (EAF), dimethylethylammonium formate (DMEAF), and ethylammonium hydrogensulfate (EAHS) were synthesized via the dropwise addition of equimolar quantities of the appropriate acid to the amine solutions while the temperature was maintained between 0 and 5 °C, as described previously.[2] The protic ILs ethylammonium thiocyanate (EASCN) and butylammonium thiocyanate (BASCN) were prepared from 40 wt % solutions of ammonium thiocyanate, to which an excess of the appropriate amine was added; then the solutions were refluxed at 80 °C for several days, as described previously.[55] The synthesized protic ILs, excluding the formate based protic ILs, were dried first under vacuum at ∼45 °C for several hours before heating at ∼110 °C under nitrogen purge for ∼8 h. The formate protic ILs were dried over several days under high vacuum at room temperature as excess heating promotes reaction between the cation and the anion to yield an amide. The final water content of the protic ILs was less than 1000 ppm as determined by Karl Fischer titration. Octanol used to produce PAN/octanol mixtures was purchased from Sigma-Aldrich (≥99%) and used as received.

Thermal conductivity was measured with a KD2 Pro Thermal Properties Analyzer (Decagon Devices, Inc.). The measurements are based on the transient hot-wire method (THW), using a single needle sensor (1.3 mm diameter and 60 mm long) containing both a heating element and a thermal resistor. Through heating of the sensor while simultaneously monitoring the temperature variation the thermal conductivity of the sample is calculated based on a modified version of the Carslaw and Jaeger model for an infinite line heat source. The THW has previously been shown to be effective for the measurement of IL thermal conductivity.[56] When taking measurements the needle was inserted vertically into the sample to minimize free convection induced by thermal gradients and suspended in a water bath set to the desired temperature. Once the sample had equilibrated to the desired temperature 10−15 measurements were made. The temperature of the sample at the time of measurement is also recorded by the KD2 probe using a platinum resistance probe.

Viscosity was measured for EAHS and BASCN with a TA Instruments AR-G2 rheometer using the cone and plate arrangement with a cone of 40 mm radius and angle of

1°59′36″. Temperature was controlled with a Peltier plate and jacket with chilled water.

Surface tensions of BASCN and DMEAF were determined by the pendant drop method using a Dataphysics OCA20 optical tensiometer. An image of a drop a volume of liquid suspended from a capillary was captured using a charge coupled device camera. The surface tension was then calculated by fitting the Young−Laplace equation to the drop image with use of SCA20 software

RESULTS AND DISCUSSION

Table 1 presents the thermal conductivity at 293 K for the nine protic ILs along with key physicochemical properties. Thermal conductivities range between 0.20 and 0.30 $W{\cdot}m^{-1}{\cdot}K^{-1}$, except for BASCN which has a thermal conductivity of 0.181 $W{\cdot}m^{-1}{\cdot}K^{-1}$. These thermal conductivities are higher than for common organic liquids (e.g., toluene, benzene, ethanol, etc.), which are typically 0.10−0.18 $W{\cdot}m^{-1}{\cdot}K^{-1}$, but lower than that of extensively hydrogen bonded liquids like water (0.609 $W{\cdot}m^{-1}{\cdot}K^{-1}$) and ammonia (0.507 $W{\cdot}m^{-1}{\cdot}K^{-1}$). The thermal conductivities of these protic ILs are also larger than those reported for aprotic ILs, the majority of which fall in the range of 0.13−0.17 $W{\cdot}m^{-1}{\cdot}K^{-1}$,[16−20] similar to oils. This is likely due to the absence of extensive H-bonding networks in aprotic ILs.

Previous studies have determined predictive expressions for the thermal conductivity of aprotic ILs using molar mass (M), viscosity (η), density (ρ), and melting points (T_m) in various combinations.[18,19,57−63] However, these expressions failed to describe the thermal conductivity for the protic ILs investigated here. This is likely because of differences in the interactions between ions in protic and aprotic ILs; hydrogen bonding is more prevalent in protic ILs, and $\pi-\pi$ stacking occurs in aromatic (e.g., imidazolium-based) aprotic ILs. These different interactions mean that correlations between thermal conductivity and other physicochemical properties will differ for the two IL types, so the models for aprotic ILs are not applicable for protic ILs.

Protic IL thermal conductivity does not vary consistently with the physical properties in Table 1. The absence of a relationship between viscosity and thermal conductivity is not surprising because diffusive contributions are minor in liquids. Rather, thermal transport in liquids is dominated by the strength of potential field interactions between the atoms of the molecules and ions in a liquid. This means that thermal conductivity should increase with the density of a sample. For the protic ILs investigated, denser ILs do tend to be more thermally conductive, but not invariably; density is not the only factor.

Melting points have also been used to derive predictive expressions for IL thermophysical properties, including thermal conductivity.[58,60] It is reasonable to expect correlations between T_m and thermal conductivity as both depend strongly on the strength of interatomic interactions. However, as with other physicochemical properties, there is no clear trend in Table 1 relating thermal conductivity and T_m. Similarly, surface tension (γ) is closely tied to the cohesive energy density of a liquid, and surface tension is used in expressions that describe acoustic velocity in both molecular liquids[68] and ILs.[69] The propagation of acoustic waves and heat are closely related, dictated chiefly by the potential field interactions between liquid molecules as they oscillate within a cage formed by adjacent solvating molecules. The liquid acoustic velocity features in the Bridgman equation for thermal conductivity, one of the earliest relationships reported.[70] In Table 1, there is a trend toward higher thermal conductivities with increasing surface tension, but as with density, the trend is not consistent across the protic ILs.

Thermal conductivity decreases as the cation alkyl chain length is increased for a given anion, e.g. $\lambda_{BAN} < \lambda_{PAN} < \lambda_{EAN}$. Similarly, attaching additional $-CH_3$ moieties to the amine N atom in the dimethylethylammonium cation ($DMEA^+$) decreases thermal conductivity. In contrast, for a given alkyl chain length, changing the anion produced relatively small changes in thermal conductivity; the thermal conductivities of EAF, EAN, and EAHS are 0.249, 0.245, and 0.259 $W{\cdot}m^{-1}{\cdot}K^{-1}$, respectively. These results are opposite to those measured for the speed of sound in imidazolium-based ILs, which depend strongly on the anion structure, and are relatively insensitive to cation alkyl chain length.[57] (The thermal conductivity of EASCN, however, is notably lower at 0.209 $W{\cdot}m^{-1}{\cdot}K^{-1}$. The reason for this specific anion effect is discussed below.)

The relationship between alkyl chain length and thermal conductivity can be rationalized by using the pseudolattice phonon-hopping model[43] and known IL liquid nanostructures.[2,26,65] In the Bahe−Varela model, the phonon-like vibrations are generated in the ordered polar domains, and the proportion of vibration modes able to participate in phonon-hopping is limited by the uncorrelated regions, which act as barriers whose conductance is essentially determined by their spatial dimensions, among other characteristics.[43] Like their aprotic counterparts, protic IL nanostructure consists of charged and uncharged domains. Charged domains are more strongly ordered than uncharged domains due to strong electrostatic and hydrogen bonding interactions producing well-defined arrangements of anions around cation charge groups, while alkyl chain regions are less well ordered, as revealed by the radial distribution functions.[65] The charged and uncharged regions of the IL nanostructure thus define the correlated and uncorrelated (respectively) domains used in the Bahe−Varela model. Support for this designation is provided by previous studies of IL acoustic properties, which confirm that polar domains in these systems are stiffer than the apolar ones.[42]

Neutron diffraction experiments and model fitting have shown that the underlying bulk nanostructure is retained, and ion arrangements in the polar domain are essentially unchanged, as alkyl chain length is increased.[2,21,26,65] However, the bulk liquid correlation length (determined from low q Bragg peaks) increases with cation alkyl chain length due to the thickness of the apolar domain increasing. Thus, increasing the cation alkyl chain length decreases thermal conductivity in two ways. First, the larger apolar domains present a greater barrier to phonon hopping. Second, the volume fraction of the more thermally conductive polar domain is decreased via a "dilution effect".

All of the protic ILs studied here have sponge-like bulk nanostructure except EtAN and DMEAF. The nanostructure of EtAN consists of small clusters of polar and apolar groups, which at first glance may be expected to be less thermally conductive than the well-structured ILs. However, the alcohol group on the end of the cation alkyl chain gives rise to more extensive hydrogen bonding in EtAN, which is generally associated with higher thermal conduction, and the small apolar domains mean the barriers to phonon hopping are relatively low; clearly it is not a requirement that the polar domains are continuous for effective thermal conduction. This argument

also accounts for the relatively high (compared to an aprotic IL) thermal conductivity of DMEAF, which is known to have weak nanostructure,[71] and is more like a classical molten salt. Thermal conduction occurs via phonon hopping between charged groups which are separated by the hydrocarbon moieties. Compared to the more strongly structured ILs, correlations between charged groups are weak, and DMEAF cannot form a 3-dimensional hydrogen bond network. Both these factors contribute to reduced thermal conductivity.

Thermal conductivities of protic ILs with thiocyanate anions are lower than for the same cation with nitrate, formate, and hydrogen sulfate anions, despite the bulk nanostructures also being sponge-like in SCN^- ILs. This could be because fewer vibrational modes are available for thermal conduction compared to the other ILs or hydrogen bonds in SCN^- ILs are less effective for thermal conduction because sulfur is acting as an acceptor atom, as opposed to oxygen in all the other ILs.

In previous work on the thermal conductivity of $HmimPF_6$ and $BmimBF_4$, Carrete et al.[43] used $\omega_C = 2\pi c_S/a$ to approximate the cutoff frequency for modes able to hop across the barriers of the uncorrelated domains, where c_S is the IL acoustic velocity and a is the distance between correlated regions in the liquid. Although the authors assumed face centered cubic packing in their original calculations (as for 1:1 electrolyte solutions), for all the protic ILs investigated here, except perhaps for DMEAF, this assumption is invalid. In the sponge-like protic ILs, a is instead equated to the distance across the uncharged domain. (This approach cannot be employed for DMEAF or EtAN because the bulk nanostructures are different.) This is approximated by the length of two cation alkyl chains determined from the Tanford equation,[72] as previous studies have shown that there is minimal interdigitation of cation alkyl chains within the bulk sponge nanostructure; the similarities of the repeat spacings for the EA^+ ILs, which are 10.05 ± 0.05 Å, suggest that this approach is valid. The resulting cutoff frequencies, determined by using acoustic velocities (c_S) reported in the literature[36] or estimated from IL surface tension values,[69] are reported in Table 1. As alkyl chain length is increased the cutoff frequency is reduced, meaning that fewer wavelengths participate in phonon hopping and thermal conduction is reduced.

To confirm the validity of the phonon hopping pseudolattice approach, the effect of systematically altering nanostructure on the thermal conductivity of PAN by added octanol *or* added water was investigated. Previous structural studies have shown that water selectively swells the PAN charged domain,[73,74] while octanol swells the uncharged regions up to a certain concentration before the nanostructure breaks and a homogeneous solution results.[73,75] For addition of water to PAN, the sponge nanostructure remains intact until the water concentration is greater than ~75 mol %. For addition of octanol to PAN, the sponge nanostructure remains intact until the octanol concentration is greater than ~50 mol %.[75] If liquid nanostructure provides the barriers to heat transfer, the rate of change in thermal conductivity should have a break point at the concentration corresponding to the loss of nanostructure. The thermal conductivities at 293 K for PAN–water and PAN–octanol mixtures as a function of PAN mole fraction are presented in Figures 1 and 2.

Small-angle X-ray scattering has shown that addition of water to PAN at low concentrations results in swelling of the polar domains.[73] This is consistent with Figure 1, where the thermal conductivity increases gently with addition of water at

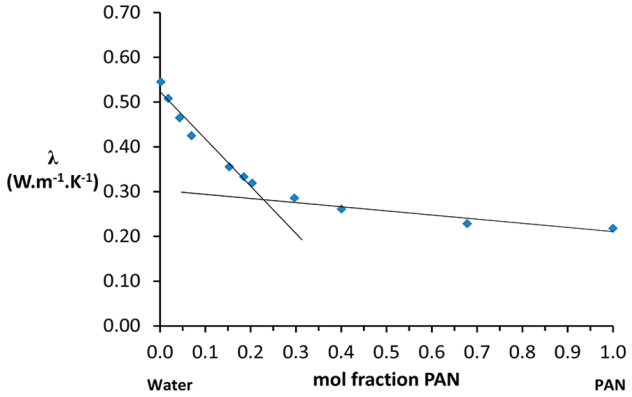

Figure 1. Thermal conductivity versus mole fraction of PAN for PAN–water mixtures at 293 K. Data are shown with blue diamonds; the black lines are added as visual guides.

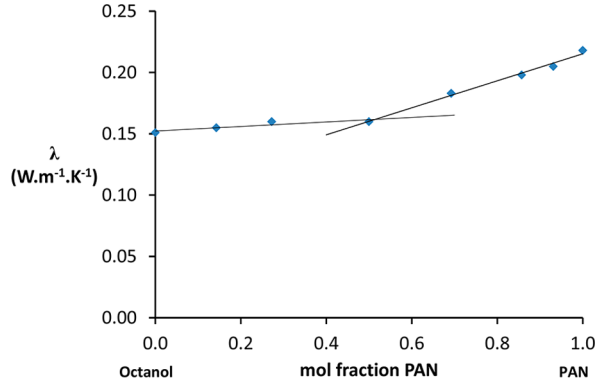

Figure 2. Thermal conductivity versus mole fraction of PAN for PAN–octanol mixtures at 293 K. Data are shown with blue diamonds; the black lines are added as visual guides.

concentrations below ~75 mol %. This increase is a consequence of water having a higher thermal conductivity than PAN and the polar domain volume fraction increasing with added water. Above 75 mol % water the sponge structure of PAN breaks down, resulting in a concentrated salt solution.[73] The thermal conductivity increases rapidly above this concentration, resulting in a break point in the thermal conductivity. The rapid increase in the thermal conductivity above 75 mol % water occurs because the barriers to thermal conduction provided by the uncharged domains have been eliminated. Now, the individual water solvated ions of the IL provide the (small) barriers to thermal conduction. As their concentration is reduced, the thermal conductivity increases until that of pure water is reached. These results are consistent with those obtained previously for mixtures of $BmimBF_4$–water and $HmimPF_6$–ethanol.[43] An early investigation into the effect of water addition on IL thermal properties concluded that water produced a lower than expected change in measured thermal conductivity.[56] The reason for this finding is made clear by the present work. Even at high water concentrations (i.e., 20 mol %) the IL–water mixture retains structural features of the pure IL which impose barriers to thermal transport.

The addition of octanol to PAN decreases thermal conductivity. This is because octanol swells the nonpolar domains of PAN impeding phonon hopping (i.e., the cutoff frequency is reduced) and thermal conductivity decreases. Initially, thermal conductivity decreases rapidly with octanol concentration due to the increasingly large barriers to phonon

dx.doi.org/10.1021/jp507408r | J. Phys. Chem. B 2014, 118, 12017–12024

propagation. Similar to PAN−water, there is a sharp transition in the rate of change in thermal conductivity with octanol concentration. This breakpoint occurs at ∼50 mol % octanol, the same concentration as X-ray scattering experiments have shown that the nanostructure of PAN is lost resulting in a solution of cations and anions in octanol.[75] Addition of more octanol further dilutes these ions, and thermal conductivity steadily decreases to the pure octanol limit.

Thermal conductivity depends weakly on temperature for the pure protic ILs examined cf. Figure 3. Weak thermal

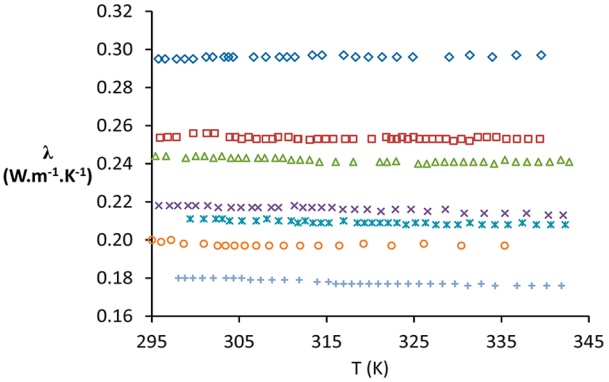

Figure 3. Thermal conductivity as a function of temperature (T) for EtAN (blue diamonds), EAHS (red squares), EAN (green triangles), PAN (purple crosses), EASCN (blue asterisks), BAN (orange circles), and BASCN (blue +'s).

conductivity−temperature dependencies are common as increasing the temperature has only a small effect on the interactions between a liquid's atoms and vibrational modes.[44] This result is predicted by the Bahe−Varela theory for ILs, which assumes a Debye density of states for phonons in the ordered regions, $g(\omega) \propto \omega^2/\omega_D{}^3$, and constant hopping probability across the barriers for phonon-like vibrations with frequencies lower than a critical cutoff, $\omega_c = 2\pi c_s/a$. The consistency of the model predictions with experimental results for aprotic ILs[43] confirms the validity of these assumptions. However, for most liquids, thermal conductivity decreases with temperature because the increased thermal motion of liquid molecules introduces anharmonicity to the vibrational modes that facilitate thermal transport, giving rise to extensive phonon−phonon dispersion in the ordered regions.[43,44]

Like most other liquids,[76] the thermal conductivity of the protic ILs decreases weakly with temperature, except for EtAN, which increases gently. Few other liquids exhibit increases in thermal conductivity with temperature aside from water,[77] where the thermal conductivity increases with temperature before reaching a maximum (at ∼350−360 K[77]), then decreases at higher temperatures. This increase in thermal conductivity with temperature is thought to be a consequence of water's dense H-bond network. The hydrogen bond network is denser in EtAN than for the other protic ILs because the alcohol group provides an additional donor and acceptor site. This dense hydrogen bond network likely leads to higher heat conduction with temperature in a similar fashion as for water. To the best of our knowledge, increasing thermal conductivity with temperature has not previously been reported for an IL.

Indeed, the increasing thermal conductivity for densely hydrogen bonded liquids like EtAN can be explained within the framework of Bahe−Varela theory. According to this theory, where the phonon-like vibrations have a quasi-Debye spectrum and frequency-independent transmission probability up to the frequency cutoff, the conductivity of the disordered barriers is given by[43]

$$G_{ij} = \frac{514\pi k_B}{\hbar^2} N_i N_j \frac{\alpha \omega_T{}^5}{\omega_D{}^6} \Xi\left(\frac{\omega_c}{2\omega_T}\right)$$

$$\hbar\omega_T = k_B T \Xi(x) = \int_0^x \frac{y^6}{\sinh^6 y}\, dy \quad (1)$$

where N_i is the number of particles in domain i, ω_D is the Debye frequency, ω_T is the thermal frequency, α is the hopping probability,[43] and k_B is Boltzmann's constant. For imidazolium-based ILs that do not have hydrogen bond networks at ambient temperature, it is enough to expand the integrand of the function $\Xi(x)$ to the lowest order,[43] and therefore $\Xi(\omega_c/2\omega_T) \approx (\omega_c/2\omega_T)^5$. This implies that the thermal conductivity of the system with domains of characteristic length l,

$$\kappa = \frac{G_0}{l}\left(\frac{\omega_T}{\omega_D}\right)\chi\left(\frac{\omega_c}{2\omega_T}\right), \quad G_0 = \frac{858 N_0{}^2 \pi^7 \alpha k_B}{7\hbar^2 \omega_D}, \quad \chi(x) = \frac{42}{\pi^6}\Xi(x) \quad (2)$$

is temperature independent but for anharmonicity effects.[43] However, insofar as thermal transport is concerned, the main effect of hydrogen bonding is to increase the stiffness of the ordered regions. This reinforcement of the interactions in the ordered regions associated with the existence of a hydrogen bonded network has a double effect on the vibrational spectrum: on the one side, it blue-shifts the frequency of phonon-like vibrations in the low-frequency regime, and on the other, it incorporates part of the disordered barriers (the cation polar heads and hydroxyls in EtAN) into the ordered region through the hydrogen bond network, therefore decreasing the effective width of the barriers. Both effects lead to an enhancement of the thermal conductivity of the liquid that can be modeled by an increase in the cutoff frequency for phonon hopping, ω_c. Hence, we must retain higher orders in the expansion of the integrand of the function $\Xi(x)$ in eq 1 to calculate the conductivity of the barriers in the general case, especially for liquids with dense hydrogen bonding. Thus, $\Xi(x) \approx x^5/5 - x^6/18$ and eq 2 leads to

$$\kappa \approx \frac{G_0}{l}\left(\frac{\omega_T}{\omega_D}\right)^5 \frac{42}{\pi^6}\left[\frac{1}{5}(\omega_c/2\omega_T)^5 - \frac{1}{18}(\omega_c/2\omega_T)^6\right] = \frac{G_0}{l}\left(\frac{\omega_c}{\omega_D}\right)^5 \frac{42}{32\pi^6}\left[\frac{1}{5} - \frac{\omega_c\hbar}{36 k_B T}\right] \quad (3)$$

which is of the form $\kappa(T) \approx A - B/T$, predicting an increase of thermal conduction with temperature in extensively hydrogen bonded liquids like EtAN up to a high-temperature limit. Moreover, B must be an increasing function of the degree of hydrogen bonding since ω_c increases with this parameter following the reduction of the spatial width of the disordered regions. Because B is proportional to $(\omega_c)^6$ and l^{-1} increases in thermal conduction are only observed for small, strongly hydrogen bonded structures, otherwise anharmonicity is the

dx.doi.org/10.1021/jp507408r | J. Phys. Chem. B 2014, 118, 12017−12024

dominant effect. This is why increases in thermal conduction with temperature are only observed for EtAN and not the other protic ILs, which have large, less strongly hydrogen bonded structures.

CONCLUSIONS

The thermal conductivity of nine protic ILs has been measured and analyzed with use of the Bahe−Varela pseudolattice theory. Thermal conductivity is dependent on the bulk nanostructure of the IL. For the ILs investigated, all but EtAN and DMEAF have a sponge-like nanostructure consisting of percolating polar and apolar domains. Thermal conduction occurs primarily via phonon hopping between the polar regions across the apolar domains, which act as barriers. Increasing the cation alkyl chain length increases the dimensions of the apolar domain while the polar domain structure is unaffected. This increases the barriers to phonon hopping reducing the thermal conductivity.

Thermal conductivity is highest for EtAN. This is attributed to EtAN having a denser hydrogen bond network and different nanostructure; bulk EtAN has a clustered morphology with relatively weakly formed apolar regions that provide less resistance to phonon hopping compared to the more strongly structured liquids. Thermal conductivity is weakly dependent on the IL anion, except for thiocyanate; thiocyanate ILs have the lowest thermal conductivity. The precise reason for this is currently unclear, but it may be related to reduced availability of the vibrational modes that enable phonon hopping, or hydrogen bonding, as it is only in thiocyanate ILs that sulfur acts as a H-bond acceptor.

Sharp transitions are observed for thermal conductivity versus composition in PAN−water and PAN−octanol mixtures. Breakpoints occur at concentrations corresponding to the loss of nanostructure when these solvents are mixed with the PAN. The thermal conductivity of the protic ILs decreases slightly with temperature, which is typical of most liquids. The exception is EtAN, where the conductivity gently increases. This behavior is unusual, but is well-known to occur in water. Like water, EtAN has a dense hydrogen bond network, which is likely the origin of this result. The Bahe−Varela formalism can explain this behavior qualitatively. Increased hydrogen bonding enhances structure in ordered regions, which blue-shifts the phonon-like spectrum and increases the cutoff frequency for phonon hopping.

AUTHOR INFORMATION

Corresponding Author

*E-mail: rob.atkin@newcastle.edu.au.

Notes

The authors declare no competing financial interest.

ACKNOWLEDGMENTS

This work was support by an Australian Research Council Discovery Projects. T.M. thanks the University of Newcastle for a Ph.D. stipend. R.A. thanks the ARC for a Future Fellowship.

REFERENCES

(1) Greaves, T. L.; Drummond, C. J. Protic ionic liquids: Properties and applications. *Chem. Rev.* **2008**, *108* (1), 206−237.

(2) Hayes, R.; Imberti, S.; Warr, G. G.; Atkin, R. Amphiphilicity determines nanostructure in protic ionic liquids. *Phys. Chem. Chem. Phys.* **2011**, *13* (8), 3237−3247.

(3) Hayes, R.; Warr, G. G.; Atkin, R. At the interface: solvation and designing ionic liquids. *Phys. Chem. Chem. Phys.* **2010**, *12* (8), 1709−1723.

(4) Wilkes, J. S. A short history of ionic liquids - from molten salts to neoteric solvents. *Green Chem.* **2002**, *4* (2), 73−80.

(5) Hallett, J. P.; Welton, T. Room-Temperature Ionic Liquids: Solvents for Synthesis and Catalysis. 2. *Chem. Rev.* **2011**, *111* (5), 3508−3576.

(6) Petkovic, M.; Seddon, K. R.; Rebelo, L. P. N.; Pereira, C. S. Ionic liquids: a pathway to environmental acceptability. *Chem. Soc. Rev.* **2011**, *40* (3), 1383−1403.

(7) Earle, M. J.; Seddon, K. R. Ionic liquids. Green solvents for the future. *Pure Appl. Chem.* **2000**, *72* (7), 1391−1398.

(8) Rogers, R. D.; Seddon, K. R. Ionic liquids - Solvents of the future? *Science* **2003**, *302* (5646), 792−793.

(9) Galinski, M.; Lewandowski, A.; Stepniak, I. Ionic liquids as electrolytes. *Electrochim. Acta* **2006**, *51* (26), 5567−5580.

(10) Armand, M.; Endres, F.; MacFarlane, D. R.; Ohno, H.; Scrosati, B. Ionic-liquid materials for the electrochemical challenges of the future. *Nat. Mater.* **2009**, *8* (8), 621−629.

(11) Endres, F.; El Abedin, S. Z. Air and water stable ionic liquids in physical chemistry. *Phys. Chem. Chem. Phys.* **2006**, *8* (18), 2101−2116.

(12) Angell, C. A.; Byrne, N.; Belieres, J.-P. Parallel developments in aprotic and protic ionic liquids: Physical chemistry and applications. *Acc. Chem. Res.* **2007**, *40* (11), 1228−1236.

(13) Earle, M. J.; Esperanca, J.; Gilea, M. A.; Lopes, J. N. C.; Rebelo, L. P. N.; Magee, J. W.; Seddon, K. R.; Widegren, J. A. The distillation and volatility of ionic liquids. *Nature* **2006**, *439* (7078), 831−834.

(14) Keskin, S.; Kayrak-Talay, D.; Akman, U.; Hortacsu, O. A review of ionic liquids towards supercritical fluid applications. *J. Supercrit. Fluids* **2007**, *43* (1), 150−180.

(15) Holbrey, J. D.; Reichert, W. M.; Reddy, R. G.; Rogers, R. D. Heat capacities of ionic liquids and their applications as thermal fluids. In *Ionic Liquids as Green Solvents: Progress and Prospects*; Rodgers, R. D., Seddon, K. R., Eds.; American Chemical Society: Washington, DC, 2003; Vol. *856*, pp 121−133.

(16) Fredlake, C. P.; Crosthwaite, J. M.; Hert, D. G.; Aki, S.; Brennecke, J. F. Thermophysical properties of imidazolium-based ionic liquids. *J. Chem. Eng. Data* **2004**, *49* (4), 954−964.

(17) Liu, H. J.; Maginn, E.; Visser, A. E.; Bridges, N. J.; Fox, E. B. Thermal and Transport Properties of Six Ionic Liquids: An Experimental and Molecular Dynamics Study. *Ind. Eng. Chem. Res.* **2012**, *51* (21), 7242−7254.

(18) Rausch, M. H.; Krzeminski, K.; Assenbaum, D.; Wasserscheid, P.; Leipertz, A.; Froba, A. P. Measurement and Prediction of the Thermal Conductivity of Ionic Liquids. *Chem. Eng. Technol.* **2011**, *83* (9), 1510−1514.

(19) Kanduc, M.; Naji, A.; Forsman, J.; Podgornik, R. Attraction between neutral dielectrics mediated by multivalent ions in an asymmetric ionic fluid. *J. Chem. Phys.* **2012**, *137* (17), 174704.

(20) Ge, R.; Hardacre, C.; Nancarrow, P.; Rooney, D. W. Thermal conductivities of ionic liquids over the temperature range from 293 to 353 K. *J. Chem. Eng. Data* **2007**, *52* (5), 1819−1823.

(21) Hayes, R.; Imberti, S.; Warr, G. G.; Atkin, R. Pronounced sponge-like nanostructure in propylammonium nitrate. *Phys. Chem. Chem. Phys.* **2011**, *13* (30), 13544−13551.

(22) Atkin, R.; Warr, G. G. The smallest amphiphiles: Nanostructure in protic room-temperature ionic liquids with short alkyl groups. *J. Phys. Chem. B* **2008**, *112* (14), 4164−4166.

(23) Hayes, R.; Imberti, S.; Warr, G. G.; Atkin, R. The Nature of Hydrogen Bonding in Protic Ionic Liquids. *Angew. Chem., Int. Ed.* **2013**, *52* (17), 4623−4627.

(24) Triolo, A.; Russina, O.; Bleif, H. J.; Di Cola, E. Nanoscale segregation in room temperature ionic liquids. *J. Phys. Chem. B* **2007**, *111* (18), 4641−4644.

(25) Hardacre, C.; Holbrey, J. D.; Mullan, C. L.; Youngs, T. G. A.; Bowron, D. T. Small angle neutron scattering from 1-alkyl-3-methylimidazolium hexafluorophosphate ionic liquids ([C(n)mim][PF6], n = 4, 6, and 8. *J. Chem. Phys.* **2010**, *133* (7), 7.

(26) Greaves, T. L.; Kennedy, D. F.; Mudie, S. T.; Drummond, C. J. Diversity Observed in the Nanostructure of Protic Ionic Liquids. *J. Phys. Chem. B* **2010**, *114* (31), 10022−10031.
(27) Urahata, S. M.; Ribeiro, M. C. C. Structure of ionic liquids of 1-alkyl-3-methylimidazolium cations: A systematic computer simulation study. *J. Chem. Phys.* **2004**, *120* (4), 1855−1863.
(28) Wang, Y. T.; Voth, G. A. Unique spatial heterogeneity in ionic liquids. *J. Am. Chem. Soc.* **2005**, *127* (35), 12192−12193.
(29) Lopes, J.; Padua, A. A. H. Nanostructural organization in ionic liquids. *J. Phys. Chem. B* **2006**, *110* (7), 3330−3335.
(30) Greaves, T. L.; Drummond, C. J. Solvent nanostructure, the solvophobic effect and amphiphile self-assembly in ionic liquids. *Chem. Soc. Rev.* **2013**, *42* (3), 1096−1120.
(31) Greaves, T. L.; Kennedy, D. F.; Kirby, N.; Drummond, C. J. Nanostructure changes in protic ionic liquids (PILs) through adding solutes and mixing PILs. *Phys. Chem. Chem. Phys.* **2011**, *13* (30), 13501−13509.
(32) Padua, A. A. H.; Gomes, M. F.; Lopes, J. Molecular solutes in ionic liquids: A structural, perspective. *Acc. Chem. Res.* **2007**, *40* (11), 1087−1096.
(33) Smith, J. A.; Webber, G. B.; Warr, G. G.; Atkin, R. Rheology of Protic Ionic Liquids and Their Mixtures. *J. Phys. Chem. B* **2013**, *117* (44), 13930−13935.
(34) Burrell, G. L.; Dunlop, N. F.; Separovic, F. Non-Newtonian viscous shear thinning in ionic liquids. *Soft Matter* **2010**, *6* (9), 2080−2086.
(35) Takada, A.; Imaichi, K.; Kagawa, T.; Takahashi, Y. Abnormal viscosity increment observed for an ionic liquid by dissolving lithium chloride. *J. Phys. Chem. B* **2008**, *112* (32), 9660−9662.
(36) Capelo, S. B.; Mendez-Morales, T.; Carrete, J.; Lago, E. L.; Vila, J.; Cabeza, O.; Rodriguez, J. R.; Turmine, M.; Varela, L. M. Effect of Temperature and Cationic Chain Length on the Physical Properties of Ammonium Nitrate-Based Protic Ionic Liquids. *J. Phys. Chem. B* **2012**, *116* (36), 11302−11312.
(37) Segura, J. J.; Elbourne, A.; Wanless, E. J.; Warr, G. G.; Voitchovsky, K.; Atkin, R. Adsorbed and near surface structure of ionic liquids at a solid interface. *Phys. Chem. Chem. Phys.* **2013**, *15* (9), 3320−3328.
(38) Wakeham, D.; Nelson, A.; Warr, G. G.; Atkin, R. Probing the protic ionic liquid surface using X-ray reflectivity. *Phys. Chem. Chem. Phys.* **2011**, *13* (46), 20828−20835.
(39) Niga, P.; Wakeham, D.; Nelson, A.; Warr, G. G.; Rutland, M.; Atkin, R. Structure of the Ethylammonium Nitrate Surface: An X-ray Reflectivity and Vibrational Sum Frequency Spectroscopy Study. *Langmuir* **2010**, *26* (11), 8282−8288.
(40) Ueno, K.; Watanabe, M. From Colloidal Stability in Ionic Liquids to Advanced Soft Materials Using Unique Media. *Langmuir* **2011**, *27* (15), 9105−9115.
(41) Smith, J. A.; Werzer, O.; Webber, G. B.; Warr, G. G.; Atkin, R. Surprising Particle Stability and Rapid Sedimentation Rates in an Ionic Liquid. *J. Phys. Chem. Lett.* **2010**, *1* (1), 64−68.
(42) Ribeiro, M. C. C. High-frequency acoustic modes in an ionic liquid. *J. Chem. Phys.* **2013**, *139* (11), 114505/1−114505/8.
(43) Carrete, J.; Mendez-Morales, T.; Garcia, M.; Vila, J.; Cabeza, O.; Gallego, L. J.; Varela, L. M. Thermal Conductivity of Ionic Liquids: A Pseudolattice Approach. *J. Phys. Chem. C* **2012**, *116* (1), 1265−1273.
(44) Gaeta, F. S.; Albanese, C.; Mita, D. G.; Peluso, F. Phonons in liquids, Onsagers reciprocal relations, and the heats of transport. *Phys. Rev. E* **1994**, *49* (1), 433−444.
(45) Chapman, S.; Cowling, T. G. *The Mathematical Theory of Non-uniform Gases: An Account of the Kinetic Theory of Viscosity, Thermal Conduction and Diffusion in Gases*; Cambridge University Press: New York, NY, 1970.
(46) Nasrabad, A. E.; Laghaei, R.; Eu, B. C. Molecular theory of thermal conductivity of the Lennard-Jones fluid. *J. Chem. Phys.* **2006**, *124* (8), 084506/1−084506/10.
(47) Gaeta, F. S.; Peluso, F.; Mita, D. G.; Albanese, C.; Castagnolo, D. Phonon-particle interactions and transport processes in liquids. *Phys. Rev. E* **1993**, *47* (2), 1066−1077.
(48) Chisolm, E. D.; Clements, B. E.; Wallace, D. C. Mean-atom-trajectory model for the velocity autocorrelation function of monatomic liquids. *Phys. Rev. E* **2001**, *63* (3), 031204/1−031204/6.
(49) Varela, L. M.; Garcia, M.; Sarmiento, F.; Attwood, D.; Mosquera, V. Pseudolattice theory of strong electrolyte solutions. *J. Chem. Phys.* **1997**, *107* (16), 6415−6419.
(50) Bahe, L. W. Structure in concentrated solutions of electrolytes - field-dielectric-gradient forces and energies. *J. Phys. Chem.* **1972**, *76* (7), 1062−1071.
(51) Varela, L. M.; Carrete, J.; Garcia, M.; Gallego, L. J.; Turmine, M.; Rilo, E.; Cabeza, O. Pseudolattice theory of charge transport in ionic solutions: Corresponding states law for the electric conductivity. *Fluid Phase Equilib.* **2010**, *298* (2), 280−286.
(52) Varela, L. M.; Carrete, J.; Turmine, M.; Rilo, E.; Cabeza, O. Pseudolattice Theory of the Surface Tension of Ionic Liquid-Water Mixtures. *J. Phys. Chem. B* **2009**, *113* (37), 12500−12505.
(53) Marques, M. A.; Marques, M. I. D.; Cabaco, M. I.; Gaspar, A. M.; Marques, M. P. M.; Amado, A. M.; da Costa, A. M. A. Evidence of a local order in concentrated aqueous solutions of salts constituted by ions of different valences. X-ray diffraction and Raman spectroscopy experiments. *J. Mol. Liq.* **2007**, *134* (1−3), 142−150.
(54) Bahe, L. W.; Parker, D. Activity-coefficients of 2:1 electrolytes in structured aqueous-solutions. *J. Am. Chem. Soc.* **1975**, *97* (20), 5664−5670.
(55) Coddens, M. E.; Furton, K. G.; Poole, C. F. Synthesis and gas-chromatographic stationary phase properties of alkylammonium thiocyanates. *J. Chromatogr.* **1986**, *356* (1), 59−77.
(56) Van Valkenburg, M. E.; Vaughn, R. L.; Williams, M.; Wilkes, J. S. Thermochemistry of ionic liquid heat-transfer fluids. *Thermochim. Acta* **2005**, *425* (1−2), 181−188.
(57) Frez, C.; Diebold, G. J.; Tran, C. D.; Yu, S. Determination of thermal diffusivities, thermal conductivities, and sound speeds of room-temperature ionic liquids by the transient grating technique. *J. Chem. Eng. Data* **2006**, *51* (4), 1250−1255.
(58) Shojaee, S. A.; Farzam, S.; Hezave, A. Z.; Lashkarbolooki, M.; Ayatollahi, S. A new correlation for estimating thermal conductivity of pure ionic liquids. *Fluid Phase Equilib.* **2013**, *354*, 199−206.
(59) Lynden-Bell, R. M.; Frolov, A. I.; Fedorov, M. V. Electrode screening by ionic liquids. *Phys. Chem. Chem. Phys.* **2012**, *14* (8), 2693−2701.
(60) Hezave, A. Z.; Raeissi, S.; Lashkarbolooki, M. Estimation of Thermal Conductivity of Ionic Liquids Using a Perceptron Neural Network. *Ind. Eng. Chem. Res.* **2012**, *51* (29), 9886−9893.
(61) Frost, D. S.; Dai, L. L. Molecular dynamics simulations of charged nanoparticle self-assembly at ionic liquid-water and ionic liquid-oil interfaces. *J. Chem. Phys.* **2012**, *136* (8), 084706/1−084706/6.
(62) Coutinho, J. A. P.; Carvalho, P. J.; Oliveira, N. M. C. Predictive methods for the estimation of thermophysical properties of ionic liquids. *RSC Adv.* **2012**, *2* (19), 7322−7346.
(63) Wu, K. J.; Chen, Q. L.; He, C. H. Speed of Sound of Ionic Liquids: Database, Estimation, and its Application for Thermal Conductivity Prediction. *AIChE J.* **2014**, *60* (3), 1120−1131.
(64) Poole, C. F. Chromatographic and spectroscopic methods for the determination of solvent properties of room temperature ionic liquids. *J. Chromatogr. A* **2004**, *1037* (1−2), 49−82.
(65) Hayes, R.; Imberti, S.; Warr, G. G.; Atkin, R. Effect of Cation Alkyl Chain Length and Anion Type on Protic Ionic Liquid Nanostructure. *J. Phys. Chem. C* **2014**, *118* (25), 13998−14008.
(66) Greaves, T. L.; Weerawardena, A.; Fong, C.; Krodkiewska, I.; Drummond, C. J. Protic ionic liquids: Solvents with tunable phase behavior and physicochemical properties. *J. Phys. Chem. B* **2006**, *110* (45), 22479−22487.
(67) Wakeham, D.; Eschebach, D.; Webber, G. B.; Atkin, R.; Warr, G. G. Surface composition of mixtures of ethylammonium nitrate, ethanolammonium nitrate, and water. *Aust. J. Chem.* **2012**, *65* (11), 1554−1556.
(68) Auerbach, R. Oberflächenspannung und Schallgeschwindigkeit. *Experientia* **1948**, *4* (12), 473−474.

(69) Gardas, R. L.; Coutinho, J. A. P. Estimation of speed of sound of ionic liquids using surface tensions and densities: A volume based approach. *Fluid Phase Equilib.* **2008**, *267* (2), 188−192.
(70) Horn, R. G.; Evans, D. F.; Ninham, B. W. Double-layer and solvation forces measured in a molten-salt and its mixtures with water. *J. Phys. Chem.* **1988**, *92* (12), 3531−3537.
(71) Wakeham, D.; Hayes, R.; Warr, G. G.; Atkin, R. Influence of Temperature and Molecular Structure on Ionic Liquid Solvation Layers. *J. Phys. Chem. B* **2009**, *113* (17), 5961−5966.
(72) Tanford, C. Micelle shape and size. *J. Phys. Chem.* **1972**, *76* (21), 3020.
(73) Greaves, T. L.; Kennedy, D. F.; Weerawardena, A.; Tse, N. M. K.; Kirby, N.; Drummond, C. J. Nanostructured Protic Ionic Liquids Retain Nanoscale Features in Aqueous Solution While Precursor Bronsted Acids and Bases Exhibit Different Behavior. *J. Phys. Chem. B* **2011**, *115* (9), 2055−2066.
(74) Hayes, R.; Imberti, S.; Warr, G. G.; Atkin, R. How water dissolves in protic ionic liquids. *Angew. Chem., Int. Ed.* **2012**, *51* (30), 7468−71.
(75) Jiang, H. J.; FitzGerald, P. A.; Dolan, A.; Atkin, R.; Warr, G. G. Amphiphilic Self-Assembly of Alkanols in Protic Ionic Liquids. *J. Phys. Chem. B* **2014**, *118* (33), 9983−9990.
(76) Bridgman, P. W. The Thermal Conductivity of Liquids. *Proc. Natl. Acad. Sci. U.S.A.* **1923**, *9* (10), 341−345.
(77) Ramires, M. L. V.; Decastro, C. A. N.; Nagasaka, Y.; Nagashima, A.; Assael, M. J.; Wakeham, W. A. Standard reference data for the thermal-conductivity of water. *J. Phys. Chem. Ref. Data* **1995**, *24* (3), 1377−1381.